



In vivo confocal microscopy morphological features and cyst density in Acanthamoeba keratitis

Chopra, R., Mulholland, P., & Hau, S. (Accepted/In press). In vivo confocal microscopy morphological features and cyst density in Acanthamoeba keratitis: Confocal microscopy morphology in Acanthamoeba keratitis. *American Journal of Ophthalmology*.

[Link to publication record in Ulster University Research Portal](#)

Published in:
American Journal of Ophthalmology

Publication Status:
Accepted/In press: 01/04/2020

Document Version
Author Accepted version

General rights
Copyright for the publications made accessible via Ulster University's Research Portal is retained by the author(s) and / or other copyright owners and it is a condition of accessing these publications that users recognise and abide by the legal requirements associated with these rights.

Take down policy
The Research Portal is Ulster University's institutional repository that provides access to Ulster's research outputs. Every effort has been made to ensure that content in the Research Portal does not infringe any person's rights, or applicable UK laws. If you discover content in the Research Portal that you believe breaches copyright or violates any law, please contact pure-support@ulster.ac.uk.

**In vivo confocal microscopy morphological features and cyst density in
Acanthamoeba keratitis**

Reena Chopra^{1,2} Pádraig J. Mulholland^{1,3} Scott C. Hau^{1,2}

¹NIHR Biomedical Research Centre for Ophthalmology, Moorfields Eye Hospital
NHS Foundation Trust and UCL Institute of Ophthalmology, London, United
Kingdom

²Department of Cornea and External Disease, Moorfields Eye Hospital NHS
Foundation Trust, London, United Kingdom

³Optometry and Vision Science Research Group, School of Biomedical Sciences,
Ulster University, Coleraine, United Kingdom

Short title

Confocal microscopy morphology in *Acanthamoeba* keratitis

Correspondence and reprint requests:

Scott Hau, NIHR Biomedical Research Centre at Moorfields Eye Hospital NHS
Foundation Trust and UCL Institute of Ophthalmology, London, United Kingdom.
Tel: +44 7905 295888
Email: s.hau@nhs.net

ABSTRACT

Purpose: To correlate in vivo confocal microscopy morphological features (IVCM-MF) and *Acanthamoeba* cyst density (ACD) with final best corrected visual acuity (BCVA) in *Acanthamoeba* keratitis (AK).

Design: Retrospective cohort study.

Methods: Patient demographics, treatment outcome, and corresponding IVCM-MF performed at the acute stage of infection were analysed. Inclusion criteria were microbiological positive AK cases seen at Moorfields Eye Hospital between February 2013 and October 2017. Statistical significance was assessed by multinomial regression and multiple linear regression analysis. Main outcome measures were final BCVA.

Results: A total of 157 eyes (157 patients) had AK. Absence of single file of round/ovoid objects was associated with a BCVA of 6/36 to 6/9 (OR 8.13; 95% CI, 1.55-42.56, $P = 0.013$) and $\geq 6/6$ (OR 10.50; 95% CI, 2.12-51.92, $P = 0.004$) when compared to NPL to 6/60. Absence of rod/spindle objects was associated with a BCVA of $\geq 6/6$ (OR 4.55; 95% CI, 1.01-20.45, $P = 0.048$). Deep stromal/ring infiltrate was associated with single file round/ovoid objects (OR 7.78; 95% CI, 2.69-22.35, $P < 0.001$), rod/spindle objects (OR 7.05; 95% CI, 2.11-23.59, $P = 0.002$), and binary round/ovoid objects (OR 3.45; 95% CI, 1.17-10.14, $P = 0.024$). There was a positive association between ACD with treatment duration ($\beta = 0.14$, $P = 0.049$), number of IVCM-MF ($\beta = 0.34$, $P = 0.021$) and clusters of round/ovoid objects ($\beta = 0.29$, $P = 0.002$).

Conclusions: Specific IVCM-MF correlate with ACD and clinical staging of disease, and are prognostic indicators for a poorer visual outcome.

INTRODUCTION

Acanthamoeba keratitis (AK) is a rare but potentially sight threatening infection. The organism *Acanthamoeba* is an opportunistic protozoan and it exists in two forms, an active trophozoite and a dormant cyst. The organism was first described as an ocular pathogen in 1974¹ but with the use of soft contact lenses, the incidence of AK has increased dramatically over the last two decades, especially in developed countries.² The initial presenting signs of AK can be similar to other forms of keratitis and it is often mistakenly diagnosed as herpes simplex keratitis (HSK).³ This delay in diagnosis and the potential injudicious use of topical steroids in treating presumed herpetic related inflammation, prior to anti-amoebic treatment, often results in poor visual outcome and severe inflammatory complications.³⁻⁵

Current diagnostic methods of AK include culture, polymerase chain reaction (PCR), or in vivo confocal microscopy (IVCM). Culture yields poor sensitivity with a positive result ranging from 0 to 68%, whereas the sensitivity is greater with PCR but false-negative results do occur.⁶ Various studies have shown the diagnostic accuracy of infectious keratitis with IVCM ranges from 56% to 100%,⁷⁻¹² with characteristic morphological structures unique to *Acanthamoeba* also being identified using this technique.^{6,13,14} Such features of AK have also been demonstrated to be related to clinical prognosis and outcome. Specifically, a deep location of cysts and the presence of clusters or chains of cysts have been found to be significantly associated with a poorer visual outcome, this leading to making the assumption that the location of cysts and the pattern of cyst distribution are important prognostic indicators in AK.¹⁵

The aim of this study was to correlate IVCM morphological features (IVCM-MF) and *Acanthamoeba* cyst density (ACD) with clinical staging and visual outcome in eyes cultured or polymerase chain reaction (PCR) positive for AK. In addition, we assessed the intra and inter-observer agreement in ACD estimation.

METHODS

Participants

This was a retrospective, cohort study. Ethical approval was obtained from Moorfields Eye Hospital, London, United Kingdom, Research Ethics Committee (ROAD 15/042), and it adhered to the tenets of the Declaration of Helsinki. Patients were identified using an electronic medical database consisting of patients with AK who were treated at Moorfields Eye Hospital between February 2013 to October 2017. Inclusion criteria consisted of all cultured or PCR positive cases for *Acanthamoeba*, clinical presentation consistent with AK, IVCM performed at the acute stage of the keratitis with round/cystic type lesions compatible with AK, and patients who have reached treatment completion. Treatment completion was defined as quiescence of disease for a period of 3 months or more on stopping anti-amoebic therapy. For patients with bilateral disease, the first affected eye was used for the analysis. Cases cultured positive for both *Acanthamoeba* and bacteria was classified as AK as bacteria, in general, are too small to be detected by IVCM.¹⁶ Cases that did not conform to the above criteria were excluded from the study.

Culture methods

Corneal scrapings for corneal culture were inoculated on a range of media as described previously.⁷ Culturing for *Acanthamoeba* from a cornea scrape was plated in non-nutrient agar which had been overlaid with *Escherichia coli*. All microbiological investigations were undertaken independently in an external laboratory (The Doctors Laboratory, London, UK).

Clinical examination, treatment and data collection

All patients underwent a clinical examination including Snellan visual acuity and slit lamp examination. AK corneal staging was classified into the following categories by a corneal specialist on diagnosis: 1 - epitheliitis, 2 - epitheliitis with perineural infiltrates, 3 - anterior stromal disease, 4 - deep stromal disease, and 5 - ring infiltrate.^{6,17} Scleritis associated with AK was classified to the most severe group (5 – ring infiltrate). All patients commenced on hourly anti-amoebic treatment for 5 days following diagnosis and the drugs then tapered according to clinical response. Treatment included either mono-therapy with a biguanide (polyhexamethylene biguanide or chlorhexidine gluconate) or dual therapy with a biguanide in combination with a diamidine (propamidine isethionate or hexamidine).

The following patient demographics were recorded: age, symptom duration prior to diagnosis, previous treatment prior to the diagnosis of AK, prior topical steroid use, previous diagnosis of HSK, duration of anti-amoebic therapy, surgical intervention, and final best corrected visual acuity (BCVA).

IVCM

IVCM was performed using a standard operating procedure with the Heidelberg Retina Tomograph/Rostock Cornea Module (HRT II/RCM, Heidelberg Engineering, Dossenheim, Germany) confocal microscope by trained clinicians on the day of presentation.⁷ A sterile Tomocap (Heidelberg Engineering) was mounted over the objective of the microscope and 0.2% polyacrylic acid (Viscotears, Novartis, Camberley, UK) was used as a coupling agent between the cap and the lens objective. Topical anaesthetic (0.5% proxymetacaine hydrochloride, Bausch & Lomb, Kingston-upon-Thames, UK) and 1% Carmellose sodium (Celluvisc, Allergan, Marlow, UK) was instilled into both eyes prior to the examination. The instrument was brought into contact of the eye and the central region of the corneal ulcer or infiltrate was scanned first followed by the top, left, bottom and right margin of the affected area. Multiple volumes (a series of 40 images over 80µm depth) scans of the cornea from the superficial epithelium all the way down to the endothelium were recorded. Each en face image consists of 384 x 384 pixels covering an area of 400 µm x 400 µm, providing a transverse resolution of approximately 1-2 µm.

AK image selection and classification

All available confocal images and sequences were reviewed by one experienced observer (SH) who was masked to the clinical outcome of the patients. In total, this equated to approximately 1200 images for each patient. Firstly, images were reviewed anteroposteriorly from the epithelium to endothelium and if round/ovoid, hyper-reflective objects (as defined below) were identified on one or more images then that eye was classified as IVCM positive for *Acanthamoeba*.

Secondly, images were classified into the various IVCN-MF as follow: round/ovoid hyper-reflective objects, measuring 10-25 μm , without double wall; round/ovoid hyper-reflective objects, measuring 10-25 μm , with double wall; target sign - round/ovoid hyper-reflective central object, measuring 10-25 μm , with surrounding halo; signet ring - round hyper-reflective outer ring, measuring 10-25 μm , with a grey/dark center; cluster of round/ovoid hyper-reflective objects; hyper-reflective polygonal/stellate-type objects; binary round/ovoid hyper-reflective objects; trophozoite-like hyper-reflective objects, measuring 25-40 μm , with spindle shape projection from its surface suggestive of acanthopodia; single file or linear chains of round/ovoid hyper-reflective objects; coffee bean shape hyper-reflective objects; large hyper-reflective objects >30 μm in size; and rod/spindle-shape hyper-reflective objects.^{6,18-20} Figure 1 shows the images of the various IVCN-MF classifications. Host inflammatory cellular features including the type of inflammatory cellular response; non- dendritiform cells (NDCs), dendritiform cells (DCs) or mixed,²¹⁻²³ and whether the subbasal nerve plexus (SBNP) and keratocytes were visible or not, were also recorded. We defined DCs as bright specular structures with processes measuring up to 55 μm in size and NDCs as irregular hyper-reflective structures measuring 10 to 40 μm in diameter without any dendritic form processes.²¹⁻²³

ACD estimation

ACD estimation was performed by two experienced observers in assessing keratitis with IVCN: observer 1 (RC) has 7 years and observer 2 (SH) has 16 years of experience, respectively. Cyst counting was performed independently in a masked fashion by each observer and only images taken centrally from the cornea ulcer/infiltrate were used for ACD estimation. The depth of cysts infiltration was recorded into one of the following anatomical locations: epithelium only, epithelium and anterior stroma up to 250 μm , or present in the whole cornea. For each eye, up to 10 representative images from each anatomical location where cysts were present, were selected by one observer (SH). Only images where 1) the cystic morphology features were clearly visible, 2) focus and contrast were optimal, and 3) the entire image displayed the same corneal layer en face, without distortion, were selected for analysis.²⁰

Due to the difficulties in differentiating host inflammatory cells and keratocytes from trophozoites⁷ and other non-cystic morphologies, the following features were excluded from ACD estimation: polygonal/stellate-type objects (Fig 1F), trophozoite-like objects (Fig 1H), coffee bean shape objects (Fig 1J), and large hyper-reflective objects > 30 μm in size (Fig 1K). In addition, rod/spindle objects (Fig 1L), which do not resemble *Acanthamoeba* cysts, were not used for cyst density estimation. Therefore, only the cystic morphological features (Figure 1A – E, G and I) were used for ACD estimation. From the selected images, each observer subjectively chose 3 images with the highest cyst count for ACD estimation.¹⁹ The cysts were marked manually over each 400 μm x 400 μm image, and the density determined using the proprietary built-in Cell Counting Software (cells/ mm^2) on the HRT II/RCM. If the cysts were present in more than one anatomical location then 3 images were chosen from each location (averaging 9 images per eye) and the ACD obtained by taking an average from all the images. The final mean ACD for each eye was obtained by averaging the counts between both observers.¹⁹ To assess intra- and interobserver agreement, 100 images were randomly selected and the ACD obtained over two

occasions by each observer, separated by one month apart, with the images being re-randomised between assessments.

Statistical analysis

Data analysis was performed with SPSS software (IBM SPSS Statistics V24, USA). Descriptive statistics were used to summarise patient demographic data. Bland-Altman plots were used to assess intra- and inter-observer agreement for ACD estimates.²⁴ BCVA was used as the main outcome variable and it was stratified into 3 categories: no perception of light (NPL) to 6/60 (used as the reference variable for comparison), 6/36 to 6/9, and better than or equal to (\geq) 6/6. The rationale for the visual acuity stratification was to evaluate the level of vision that would entitle a patient to be potentially registered for sight impairment in the UK, the minimum visual acuity requirement for driving a vehicle, and the attainment of a normal level of BCVA, expected in age-matched healthy individuals, on resolution of the disease. In addition, the classification was chosen to minimise unequal sample comparison that could result in artefactual findings. Multinomial regression analysis was used to estimate the odds ratio (OR) with 95% confidence intervals (CI) to assess factors associated with the worst visual outcome category of NPL to 6/60. Univariate analysis was performed first followed by multivariable analysis. A separate binary logistic regression analysis assessing morphological features with disease severity on clinical presentation as the outcome variable, categorised by epithelial/anterior stroma disease $\leq 250 \mu\text{m}$ or deep stroma disease/ring infiltrate $> 250 \mu\text{m}$ (as defined by the pachymetry measurements on IVCN) was performed. The association between various factors with ACD was analysed by univariate linear regression analysis followed by multiple linear regression analysis controlling for confounding variables. A P value of < 0.05 was considered as statistically significant.

RESULTS

A total of 171 eyes (171 patients) diagnosed with AK confirmed by culture or PCR positive for *Acanthamoeba* were identified over the study period. Of these, 14 eyes were excluded from the analysis: 4 due to equivocal diagnosis with IVCN because of poor image quality and 10 were excluded due to missing final outcome data or were lost to follow-up on completion of anti-amoebic treatment. Therefore, 157 eyes (157 patients) were included for analysis. All of the patients in this study were contact lens wearers.

Clinical characteristics and disease outcome

Patient demographics and clinical characteristics are shown in Table 1. Of the 2 eyes that needed an evisceration, one had a painful non-healing persistent epithelial defect (PED) over 6 months, and the second had recurrent corneal perforation and underwent 3 cornea transplants prior to evisceration. In total, 3 eyes were NPL, including the 2 eviscerated, and the third patient had a conjunctival autograft for PED and developed end stage secondary glaucoma. For the remaining 24 eyes in the category of NPL to 6/60, 13 (8.4%) did not receive any surgical intervention, 10 (6.5%) had one or more corneal transplant, and 2 (1.3%) had an amniotic membrane graft. For the categories of 6/36 to 6/9, and $\geq 6/6$, 7 (4.5%) had one or more corneal transplants and 2 (1.3%) had one corneal transplant, respectively. Of the 6 who

developed corneal perforation, 3 (1.9%) had a BCVA of NPL to 6/60, and 3 (1.9%) had a BCVA between 6/36 and 6/9.

Comparison of clinical characteristics and final BCVA with univariate analysis is shown in Table 2. Multivariable analysis revealed the duration of anti-amoebic treatment to show a statistically significant association with a BCVA of 6/36 to 6/9 (OR 0.83; 95% CI, 0.73 to 0.93, $P = 0.002$) and $\geq 6/6$ (OR 0.77; 95% CI, 0.67 to 0.88, $P < 0.001$) when compared to the BCVA category of NPL to 6/60. Furthermore, symptom duration < 3 weeks (OR 4.63; 95% CI, 1.03 to 21.41, $P = 0.05$), a prior diagnosis of HSK (OR 0.11; 95% CI, 0.02 to 0.86, $P = 0.035$), and absence of surgical intervention (OR 9.08; 95% CI, 1.23 to 67.19, $P = 0.03$) were associated with a BCVA of $\geq 6/6$ when compared to NPL to 6/60.

IVCM host cellular response

The SBNP was visible in 20 (12.7%) eyes where the disease was confined to the epithelium and anterior stroma. The SBNP was not visible in any of the 37 (23.6%) eyes where there was a ring infiltrate or deep stromal involvement. Similarly, keratocytes were seen more often in disease confined to the epithelium and anterior stroma compared to deep stromal disease and/or ring infiltrate: 114 (82.1%) versus 25 (17.9%), respectively. The distribution of inflammatory cell type detected include NDCs only in 51 eyes (32.5%), mixed DCs and NDCs in 99 eyes (63.1%), DCs only in 3 eyes (1.9%), and none detected in 4 eyes (2.5%). The 4 eyes where no obvious inflammatory cells were detected all had advanced disease with ring infiltrate and multiple cystic morphological features were visible throughout the central corneal stroma.

IVCM-MF and disease outcome

Comparison of the various IVCM-MF seen in AK and final BCVA on univariate analysis is shown in Table 3. In multivariable analysis, the absence of single file of round/ovoid hyper-reflective objects remained statistically significant in the association of a BCVA of 6/36 to 6/9 (OR 8.13; 95% CI, 1.55 to 42.56, $P = 0.013$) and $\geq 6/6$ (OR 10.50; 95% CI, 2.12 to 51.92, $P = 0.004$) when compared to patients in the NPL to 6/60 category. Furthermore, the absence of rod/spindle-shaped hyper-reflective objects (OR 4.55; 95% CI, 1.01 to 20.45, $P = 0.048$) was associated with a BCVA of $\geq 6/6$ when compared to NPL to 6/60. Using disease severity on clinical presentation as the outcome variable, multivariable analysis showed the presence of deep stroma/ring infiltrate to be significantly associated with single file of round/ovoid hyper-reflective objects (OR 7.78; 95% CI, 2.69 to 22.35, $P < 0.001$), rod/spindle-shape hyper-reflective objects (OR 7.05; 95% CI, 2.11 to 23.59, $P = 0.002$), and binary round/ovoid hyper-reflective objects (OR 3.45; 95% CI, 1.17 to 10.14, $P = 0.024$).

ACD

Bland-Altman plots show good intra- and inter-observer agreement with no obvious fixed or proportional bias detected for both observers, Figure 2. Multiple linear regression revealed a significant positive association between increase in ACD with duration of anti-amoebic treatment ($\beta = 0.14$, $P = 0.049$), total number of IVCM-MF ($\beta = 0.34$, $P = 0.021$) and clusters of round/ovoid hyper-reflective objects ($\beta = 0.29$, $P = 0.002$).

DISCUSSION

The presence of single file or linear chains of round/ovoid hyper-reflective objects on diagnosis was independently and strongly associated with the poorest visual outcome of NPL to 6/60 in patients with AK. This morphological feature has previously been found to be present only in patients who were PCR-positive for *Acanthamoeba*, though it was not found to be significantly associated with AK. However, the authors did comment a larger series would be needed to determine the specificity of this feature in diagnosing AK.⁶ Comparatively, our cohort is much larger and we have demonstrated that this feature is a strong predictor for a visual outcome in the range of NPL to 6/60. In addition, the presence of rod/spindle shape hyper-reflective objects was significantly associated with a visual acuity of worse than 6/9. This morphological feature has been reported in all forms of keratitis including *Acanthamoeba*, bacterial and fungal keratitis.^{6,25} De Craene et al⁶ classified rod-hyper-reflective objects separately from spindle-shape hyper-reflective objects and found the rod-shape phenotypes were seen only in PCR-positive cases whereas the spindle-shape phenotype were observed equally between PCR-positive and PCR-negative cases. From our observation, it is difficult to distinguish these two phenotypes, hence the rationale for classifying all rod/shape features in the same category. Morphologically, rod/spindle-shape objects do not resemble *Acanthamoeba* cysts or trophozoites and it is plausible that they represent the spindle-shape fibroblasts and/or myofibroblasts seen during inflammation rather than the organism itself. The replacement of keratocytes by fibroblasts and myofibroblasts causes corneal haze and scar formation, resulting in visual loss.²⁶

Round/ovoid hyper-reflective objects without double wall were identified in all eyes in the study, and therefore they were not a good prognostic indicator. This feature has been described in numerous studies to be associated with AK,^{6,10,11,15,27,28} but also seen in 51.8% of PCR-negative patients in a previous case control study.⁶ Similarly, Fust et al²⁹ found round/oval hyper-reflective objects were not specific for AK and were present in 40% of FK and 55% of BK, respectively. Although round/oval hyper-reflective objects are seen in AK, the high rate of presence in non-AK challenges the assumption that these objects are specific for AK only.²⁹ We found 3 further IVCMMF that were significantly associated with the poorest visual outcome on univariate analysis. Clusters of round/ovoid hyper-reflective objects were strongly associated with the BCVA category of NPL to 6/60. These clusters are highly specific for a diagnosis of AK but low in sensitivity.⁶ Binary hyper-reflective objects and target signs were also significantly associated with the poorest visual outcome. Similarly, target signs are pathognomonic of AK with high specificity but low sensitivity.^{6,29} Furthermore, this sign has also been found to be present in over 80% of eyes with a clinical suspicion of AK.³⁰ Trophozoite-like hyper-reflective objects have been reported to be associated with AK^{29,30} with high specificity⁶ but we did not find this to be a good prognostic indicator. Round/ovoid hyper-reflective objects with double wall, large hyper-reflective objects >30µm in size, coffee bean shape hyper-reflective objects, and hyper-reflective polygonal/stellate-type objects were also observed but were not significantly associated with visual outcome due to their relatively low frequency of presence. These signs have also been reported previously by De Craene et al and were not found to be significantly associated with a diagnosis AK.⁶

Using disease severity on clinical presentation as the outcome variable, single file round/ovoid, rod/spindle-shape, and binary round/ovoid hyper-reflective objects were significantly associated with the presence of deep stroma/ring infiltrate disease. The association of single file and rod/spindle shape objects with both disease severity and the poorest visual outcome category suggest these morphological signs are important prognostic indicators in patients with AK.

We found good intra- and inter-observer agreement on cyst density estimation with no obvious systematic bias detected. The presence of cystic lesions in the stroma, a higher ACD and a greater number of different IVCM-MF were associated with the worst visual outcome category on univariate analysis. NPL to 60 eyes had nearly twice the cyst density compared to eyes with 6/36 to 6/9 and $\geq 6/6$. This is in agreement with Huang et al who found a higher cyst density and deeper cyst invasion was associated with more severe disease.¹⁹ The mean ACD on presentation found in previous studies ranges between 99 to 214 cells/mm²,^{19,20} which is higher than the mean ACD in our study even in the most severe disease group (84 cells/mm²). One possible reason for the difference is both cysts and trophozoite-like lesions were counted in the previous studies whereas only the cystic morphologies were counted in our study. Macrophages and other inflammatory cells are frequently confused with trophozoites, polygonal/stellate-type, and large hyper-reflective objects, hence the reason for only using the various cystic morphologies for ACD estimation in our study.⁷ There is a paucity of data on the usefulness of ACD estimation with anti-amoebic treatment, the difficulty of ascertaining the viability of the cysts with treatment and how long before dead cysts are removed by the host immune system, make this difficult to assess, though it has been reported that cyst density reduces by 5.3% with each month of treatment.²⁰ Furthermore, it has been found that after topical therapy, cysts demonstrating a hollow configuration existed for up to 6 months.³¹ These configurations could contribute to the variation in cystic morphology encountered in this study. However, we did not assess how cyst morphology and density changed with time or with medical therapy so further studies are needed to evaluate this.

Host keratocyte cellular response was found to be dependent on disease severity with the presence of keratocytes more commonly observed in disease confined to the epithelium/anterior stroma. Chidambaram et al found eyes with AK were less likely to have normal keratocyte-like morphology compared to other causes of microbial keratitis. This is likely to be related to the cytopathic effects on keratocytes via induction of apoptosis from direct acanthamoebae adhesion.^{32,33} Furthermore, prolonged use of anti-amoebic therapy such as polyhexamethylene biguanide and chlorhexidine can potentially cause keratocyte cell death which is dose and time dependent.³⁴

The SBNP was only seen in 12.7% of eyes and was absent in all cases of deep stromal/ring infiltrate eyes. Although quantitative analysis of the nerves was not performed, others have shown a significant drop out of nerves during the acute phase of the infection^{35,36} A strong correlation between a reduction in cornea nerves and an increase in DC density with microbial keratitis has also been demonstrated.³⁵ We found 63% of eyes had both NDCs and DCs but we have not quantitatively analysed the inflammatory cell density in this study. Previous studies have reported the density of DCs in microbial keratitis but not NDCs. Cruzat et al found AK had the

1 highest DCs in the basal epithelium whereas Chidambaram reported DCs to be the
2 highest in bacterial keratitis when compared to other forms of keratitis.^{25,35} These
3 authors cited the difference may be related to prior steroid treatment in a large
4 proportion of their patients. DCs and NDCs are merely morphological descriptions of
5 the type of presumed immune cells seen on IVCN and it is not possible, with current
6 technology, to determine the exact phenotype of these cells or to be able to
7 competently differentiate pathogenic organism from inflammatory cells.²⁵ Moreover, it
8 is not known if the inverse relationship between corneal nerves and inflammatory
9 cells seen during the acute phase of the infection with IVCN is related to direct
10 cytopathic effect from the pathogen itself on the nerves or to the severe cornea host
11 inflammatory response.^{35,36} We have not assessed recovery of the SBNP during the
12 course or on resolution of the disease but it has been shown that nerve regeneration
13 does occur during the first 6 months after resolution of the infection but it is still
14 reduced when compared to controls.³⁶

15
16
17
18 Nearly 50% of patients achieved a final BCVA of $\geq 6/6$ on resolution of the disease,
19 which is comparable to previous studies.¹⁷ Patients with ring infiltrate received anti-
20 amoebic treatment on average twice as long compared to patients with epithelial
21 disease and this is reflected by the significant association of a poorer visual outcome
22 with the longer duration of therapy. We found a shorter duration of patient symptoms
23 prior to the diagnosis of AK to be associated with a better visual outcome on
24 univariate analysis but on multivariable analysis, only the $\geq 6/6$ BCVA category was
25 significant. Our definition of symptom duration of greater or less than 3 week was the
26 same as Tu et al who found patients presenting ≥ 3 week were more likely to have
27 a final visual acuity of less than 20/25 (6/7.5) but they did not find this to be
28 statistically significant on univariate analysis, citing the subjective nature of symptom
29 onset recall by patients to be potentially unreliable.¹⁷ Although our acuity definition of
30 $\geq 6/6$ is different to the study by Tu al, our findings of an association between a
31 poorer visual outcome with symptom duration prior to diagnosis is in agreement with
32 previous studies.³⁷ We also found a prior diagnosis of HSK and the need for surgical
33 intervention were more likely to be associated with the BCVA of NPL to 6/60 when
34 compared to $\geq 6/6$ but not when compared to the category of 6/36 to 6/9 on
35 multivariable analysis. Prior diagnosis of HSK was not found to be a significant
36 predictor by Tu et al; our much lower visual acuity reference standard for comparison
37 is likely to be the reason for the difference found. Surgical intervention was
38 associated with the poorest visual outcome category, aside from the 3 eyes who
39 were NPL, 11/24 eyes needed some form of surgical intervention in this category.

40
41
42
43
44
45
46 The main limitation of our study is the retrospective design and only the first scan on
47 presentation was used for prognostication purpose. A recent study has shown that
48 monitoring ACD during treatment can be useful to assess therapeutic response, but
49 the relationship between the changes in ACD with treatment for different stages of
50 severity for AK was not assessed.²⁰ We demonstrated that disease severity on
51 presentation is associated with a higher ACD and greater number of IVCN-MF so it
52 is likely that the changes in cyst density with treatment would be different for more
53 severe disease. Further longitudinal studies are needed to evaluate the relationship
54 between ACD change with time and disease severity. Nevertheless, we have shown
55 good repeatability and reproducibility with ACD estimation when performed by
56 experienced observers, and this is important when ACD is potentially used as a
57 prognostic indicator or for disease monitoring. We based our morphological

classifications on previous publications but this process is subjective, and the difficulty in differentiating *Acanthamoeba* cysts or trophozoites from inflammatory cells, damaged epithelial cells and keratocytes, shows the limitations with current IVCM technology.^{6,7} The strengths of our study include the larger sample size, only culture or PCR positive for *Acanthamoeba* was used as the reference standard for case selection, and trained experienced observers were used for both morphological classification and ACD determination.

In conclusion, we found specific IVCM-MF correlate with ACD and clinical staging of disease on presentation and therefore, can be used as potential prognostic indicators for visual outcome in patients with AK. Further studies are required to evaluate how these morphological features evolve over the course of therapeutic treatment.

Acknowledgment/Disclosure

Funding/Support: This study was supported by Fight for Sight, UK. Reference number - 1710/1711

Financial Disclosure:

Reena Chopra receives studentship support from the College of Optometrists, United Kingdom, and is a paid intern at DeepMind.

Pádraig J. Mulholland has received travel support from Heidelberg Engineering, Germany

Scott C Hau – No financial disclosures

REFERENCES

1. Naginton J, Watson PG, Playfair TJ, McGill J, Jones BR, Steele AD. Amoebic infection of the eye. *Lancet*. 1974;2(7896):1537-1540.
2. Lee MH, Abell RG, Mitra B, Ferdinands M, Vajpayee RB. Risk factors, demographics and clinical profile of *Acanthamoeba* keratitis in Melbourne: an 18-year retrospective study. *Br J Ophthalmol*. 2018;102(5):687-691.
3. Robaei D, Carnt N, Minassian DC, Dart JK. The impact of topical corticosteroid use before diagnosis on the outcome of *Acanthamoeba* keratitis. *Ophthalmology*. 2014;121(7):1383-1388.
4. Carnt N, Robaei D, Watson SL, Minassian DC, Dart JK. The Impact of Topical Corticosteroids Used in Conjunction with Antiamoebic Therapy on the Outcome of *Acanthamoeba* Keratitis. *Ophthalmology*. 2016;123(5):984-990.
5. Carnt N, Robaei D, Minassian DC, Dart JKG. *Acanthamoeba* keratitis in 194 patients: risk factors for bad outcomes and severe inflammatory complications. *Br J Ophthalmol*. 2018;102(10):1431-1435.
6. De Craene S, Knoeri J, Georgeon C, Kestelyn P, Borderie VM. Assessment of Confocal Microscopy for the Diagnosis of Polymerase Chain Reaction-Positive *Acanthamoeba* Keratitis: A Case-Control Study. *Ophthalmology*. 2018;125(2):161-168.
7. Hau SC, Dart JK, Vesaluoma M, et al. Diagnostic accuracy of microbial keratitis with in vivo scanning laser confocal microscopy. *Br J Ophthalmol*. 2010;94(8):982-987.
8. Kanavi MR, Javadi M, Yazdani S, Mirdehghanm S. Sensitivity and specificity of confocal scan in the diagnosis of infectious keratitis. *Cornea*. 2007;26(7):782-786.

9. Tu EY, Joslin CE, Sugar J, Booton GC, Shoff ME, Fuerst PA. The relative value of confocal microscopy and superficial corneal scrapings in the diagnosis of Acanthamoeba keratitis. *Cornea*. 2008;27(7):764-772.
10. Chidambaram JD, Prajna NV, Larke NL, et al. Prospective Study of the Diagnostic Accuracy of the In Vivo Laser Scanning Confocal Microscope for Severe Microbial Keratitis. *Ophthalmology*. 2016;123(11):2285-2293.
11. Vaddavalli PK, Garg P, Sharma S, Sangwan VS, Rao GN, Thomas R. Role of confocal microscopy in the diagnosis of fungal and acanthamoeba keratitis. *Ophthalmology*. 2011;118(1):29-35.
12. Kheirkhah A, Satitpitakul V, Syed ZA, et al. Factors Influencing the Diagnostic Accuracy of Laser-Scanning In Vivo Confocal Microscopy for Acanthamoeba Keratitis. *Cornea*. 2018;37(7):818-823.
13. Matsumoto Y, Dogru M, Sato EA, et al. The application of in vivo confocal scanning laser microscopy in the management of Acanthamoeba keratitis. *Mol Vis*. 2007;13:1319-1326.
14. Parmar DN, Awwad ST, Petroll WM, Bowman RW, McCulley JP, Cavanagh HD. Tandem scanning confocal corneal microscopy in the diagnosis of suspected acanthamoeba keratitis. *Ophthalmology*. 2006;113(4):538-547.
15. Zhang X, Sun X, Jiang C, et al. A new in vivo confocal microscopy prognostic factor in Acanthamoeba keratitis. *J Fr Ophtalmol*. 2014;37(2):130-137.
16. Vaddavalli PK, Garg P, Sharma S, Thomas R, Rao GN. Confocal microscopy for Nocardia keratitis. *Ophthalmology*. 2006;113(9):1645-1650.
17. Tu EY, Joslin CE, Sugar J, Shoff ME, Booton GC. Prognostic factors affecting visual outcome in Acanthamoeba keratitis. *Ophthalmology*. 2008;115(11):1998-2003.
18. Kobayashi A, Yokogawa H, Yamazaki N, et al. In vivo laser confocal microscopy findings of radial keratoneuritis in patients with early stage Acanthamoeba keratitis. *Ophthalmology*. 2013;120(7):1348-1353.
19. Huang P, Tepelus T, Vickers LA, et al. Quantitative Analysis of Depth, Distribution, and Density of Cysts in Acanthamoeba Keratitis Using Confocal Microscopy. *Cornea*. 2017;36(8):927-932.
20. Wang YE, Tepelus TC, Gui W, Irvine JA, Lee OL, Hsu HY. Reduction of Acanthamoeba Cyst Density Associated With Treatment Detected by In Vivo Confocal Microscopy in Acanthamoeba Keratitis. *Cornea*. 2019;38(4):463-468.
21. Mastropasqua L, Nubile M, Lanzini M, et al. Epithelial dendritic cell distribution in normal and inflamed human cornea: in vivo confocal microscopy study. *Am J Ophthalmol*. 2006;142(5):736-744.
22. Postole AS, Knoll AB, Auffarth GU, Mackensen F. In vivo confocal microscopy of inflammatory cells in the corneal subbasal nerve plexus in patients with different subtypes of anterior uveitis. *Br J Ophthalmol*. 2016;100(11):1551-1556.
23. Hau S, Clarke B, Thaung C, Larkin DFP. Longitudinal changes in corneal leucocyte density in vivo following transplantation. *Br J Ophthalmol*. 2019;103(8):1035-1041.
24. Bland JM, Altman DG. Statistical methods for assessing agreement between two methods of clinical measurement. *Lancet*. 1986;1(8476):307-310.
25. Chidambaram JD, Prajna NV, Palepu S, et al. In Vivo Confocal Microscopy Cellular Features of Host and Organism in Bacterial, Fungal, and Acanthamoeba Keratitis. *Am J Ophthalmol*. 2018;190:24-33.
26. Wilson SE, Mohan RR, Mohan RR, Ambrosio R, Jr., Hong J, Lee J. The corneal wound healing response: cytokine-mediated interaction of the epithelium, stroma, and inflammatory cells. *Prog Retin Eye Res*. 2001;20(5):625-637.
27. Pfister DR, Cameron JD, Krachmer JH, Holland EJ. Confocal microscopy findings of Acanthamoeba keratitis. *Am J Ophthalmol*. 1996;121(2):119-128.
28. Alomar T, Matthew M, Donald F, Maharajan S, Dua HS. In vivo confocal microscopy in the diagnosis and management of acanthamoeba keratitis showing new cystic forms. *Clin Exp Ophthalmol*. 2009;37(7):737-739.

29. Fust A, Toth J, Simon G, Imre L, Nagy ZZ. Specificity of in vivo confocal cornea microscopy in *Acanthamoeba* keratitis. *Eur J Ophthalmol*. 2017;27(1):10-15.
30. Rezaei Kanavi M, Naghshgar N, Javadi MA, Sadat Hashemi M. Various confocal scan features of cysts and trophozoites in cases with *Acanthamoeba* keratitis. *Eur J Ophthalmol*. 2012;22 Suppl 7:S46-50.
31. Li S, Bian J, Wang Y, Wang S, Wang X, Shi W. Clinical features and serial changes of *Acanthamoeba* keratitis: an in vivo confocal microscopy study. *Eye*. 2020;34(2):327-334.
32. Takaoka-Sugihara N, Yamagami S, Yokoo S, Matsubara M, Yagita K. Cytopathic effect of *Acanthamoeba* on human corneal fibroblasts. *Mol Vis*. 2012;18:2221-2228.
33. Vemuganti GK, Sharma S, Athmanathan S, Garg P. Keratocyte loss in *Acanthamoeba* keratitis: phagocytosis, necrosis or apoptosis? *Indian J Ophthalmol*. 2000;48(4):291-294.
34. Lee JE, Oum BS, Choi HY, Yu HS, Lee JS. Cysticidal effect on *acanthamoeba* and toxicity on human keratocytes by polyhexamethylene biguanide and chlorhexidine. *Cornea*. 2007;26(6):736-741.
35. Cruzat A, Witkin D, Baniyadi N, et al. Inflammation and the nervous system: the connection in the cornea in patients with infectious keratitis. *Invest Ophthalmol Vis Sci*. 2011;52(8):5136-5143.
36. Muller RT, Abedi F, Cruzat A, et al. Degeneration and Regeneration of Subbasal Corneal Nerves after Infectious Keratitis: A Longitudinal In Vivo Confocal Microscopy Study. *Ophthalmology*. 2015;122(11):2200-2209.
37. Duguid IG, Dart JK, Morlet N, et al. Outcome of *acanthamoeba* keratitis treated with polyhexamethyl biguanide and propamidine. *Ophthalmology*. 1997;104(10):1587-1592.

LEGENDS

Figure 1.

In vivo classification of the various morphological features seen in *Acanthamoeba* keratitis.

A. Round/ovoid hyper-reflective objects, measuring 10-25 μ m, without double wall, B. Round/ovoid hyper-reflective objects, measuring 10-25 μ m, with double wall, C. Target sign - round/ovoid hyper-reflective central object, measuring 10-25 μ m, with surrounding halo, D. Signet ring - round hyper-reflective outer ring, measuring 10-25 μ m, with a grey/dark center, E. Cluster of round/ovoid hyper-reflective objects, F. Hyper-reflective polygonal/stellate-type objects, G. Binary round/ovoid hyper-reflective objects, H. Trophozoite-like hyper-reflective objects, measuring 25-40 μ m, I. Single file or linear chains of round/ovoid hyper-reflective objects, J. Coffee bean shape hyper-reflective objects, K. Large hyper-reflective objects >30 μ m in size, L. Rod/spindle-shape hyper-reflective objects.

Figure 2.

Bland-Altman plots for intra-observer and inter-observer difference against the average *Acanthamoeba* cyst density. The dash line represents the mean difference and the dotted lines indicates the 95% limits of agreement. The dark marker opacity reflects density of overlapping points. (Top) Intra-observer difference for observer 1, the mean difference is 0.13 ± 0.76 . (Middle) Intra-observer difference for observer 2, the mean difference is 0.03 ± 1.31 . (Bottom) inter-observer difference, the mean difference is 0.11 ± 1.54 .

Table 1

TABLE 1. Patient demographics and clinical characteristics (n = 157)	
Age (yrs), mean (SD , range)	41.5 (15.7, 20-81)
Sex – female, n (%)	87 (55.4)
Symptom duration prior to diagnosis (weeks), mean (SD , range)	4.7 (6.8, 0.3-56)
Previous diagnosis, n (%)	
Bacteria keratitis	47 (29.9)
Uncertain	40 (25.5)
HSV	28 (17.8)
Possible AK	35 (22.3)
Fungus	2 (1.3)
Adenovirus	2 (1.3)
Uveitis	1 (0.6)
Contact lens related abrasion	1 (0.6)
Conjunctivitis	1 (0.6)
Topical treatment prior to diagnosis of AK, n (%)	
Antibiotic	83 (52.9)
Steroid	37 (23.6)
Antiviral	28 (17.8)
Anti-amoebic	34 (21.7)
Slit lamp appearance, n (%)	
Epitheliitis	60 (38.2)
Epitheliitis with perineural infiltrate	34 (21.7)
Anterior stromal infiltrate	26 (16.6)
Deep stromal/ring infiltrate	37 (23.6)
Culture positive for acanthamoeba, n (%)	72 (45.9)
PCR positive for acanthamoeba, n (%)	120 (76.4)
Culture and PCR positive for acanthamoeba, n (%)	42 (26.8)
Duration of anti-amoebic treatment (months), mean (SD , range)	
Epithelial disease	6.9 (4.5, 1-23)
Stromal disease	9.1 (5.4, 2-27)
Ring infiltrate	14.3 (6.9, 4-24)
Final best corrected visual acuity, n (%)	
NPL to 6/60	27 (17.2)
6/36 to 6/9	55 (35)
≥ 6/6	75 (47.8)
Corneal perforation, n (%)	6 (3.8)
Surgical intervention, n (%)	
None	132 (84.1)
Corneal transplant	21 (13.4)
Amniotic membrane graft for PED	3 (1.9)
Evisceration	2 (1.3)
SD = standard deviation; AK = <i>Acanthamoeba</i> keratitis; PCR = polymerase chain reaction; PED = persistent epithelial defect	

TABLE 2. Comparison of clinical characteristics, IVCM findings, and final BCVA (n = 157)

^b Values presented as mean and standard deviation

Table 3

TABLE 3. Comparison of the various IVCN morphological features and final BCVA (n = 157)												
	BCVA NPL to 6/60 ^a (n = 27)		BCVA 6/36 to 6/9 (n = 55)		Univariate analysis			BCVA ≥ 6/6 (n = 75)		Univariate analysis		
Morphological feature	n	%	n	%	OR	95% CI	P Value	n	%	OR	95% CI	P Value
Round/ovoid hyper-reflective objects without double wall												
No	0		0		NA	NA	NA			NA	NA	NA
Yes	27	17.2	55	35.0				75	47.8			
Round/ovoid hyper-reflective objects with double wall												
No	10	12.0	32	38.6	2.37	0.92– 6.10	0.075	41	49.4	2.05	0.83– 5.06	0.12
Yes	17	23.0	23	31.1				34	45.9			
Target sign												
No	2	4.3	21	45.7	7.72	1.67– 35.99	0.009	23	50	5.53	1.21– 25.32	0.028
Yes	25	22.5	34	30.6				52	46.8			
Signet sign												
No	23	18.5	42	33.9	0.56	0.16– 1.92	0.359	59	47.6	0.64	0.19– 2.12	0.467
Yes	4	12.1	13	39.4				16	48.5			
Single file of round/ovoid hyper-reflective objects												
No	7	5.7	48	39.0	19.59	6.08– 63.15	< 0.001	68	55.3	27.76	8.69– 88.56	< 0.001
Yes	20	58.8	7	20.6				7	20.6			
Cluster of round/ovoid hyper-reflective objects												
No	7	6.3	44	39.3	11.43	3.86– 33.83	< 0.001	61	54.5	12.45	4.41– 35.16	< 0.001
Yes	20	44.4	11	24.4				14	31.1			
Trophozoite-like hyper-reflective objects												
No	21	20.2	35	33.7	0.50	0.17– 1.44	0.2	48	46.2	0.51	0.18– 1.41	0.19
Yes	6	11.3	20	37.7				27	50.8			
Rod/spindle-shape hyper-reflective objects												
No	13	9.8	48	36.4	7.39	2.47– 22.07	< 0.001	71	53.8	19.12	5.43– 67.30	< 0.001
Yes	14	56	7	28.0				4	16			
Binary round/ovoid hyper-reflective objects												
No	7	8.6	28	34.6	2.96	1.08– 8.14	0.035	46	56.8	4.53	1.70– 12.05	0.002
Yes	20	26.3	27	35.5				29	38.2			
Large hyper-reflective objects > 30µm												
No	24	18.2	45	34.1	0.56	0.14– 2.24	0.42	63	47.7	0.66	0.17– 2.53	0.54
Yes	3	12.0	10	40.0				12	48			
Coffee bean shape hyper-reflective objects												
No	27	17.5	54	35.1	NA	NA	NA	73	47.4	NA	NA	NA
Yes	0	0.0	1	33.3				2	66.7			

Polygonal/stellate objects < 30µm												
No	27	17.4	54	34.8	NA	NA	NA	74	47.7	NA	NA	NA
Yes	0	0.0	1	50.0				1	50			

BCVA = best corrected visual acuity; NPL = no perception of light; IVCM = in vivo confocal microscopy; OR = odds ratio; CI = confidence intervals; NA = not applicable - odds ratio not calculated due to very low value or value only present in one of the two binary outcome

^a NPL to 6/60 group was used as the reference for comparison

Figure 1
[Click here to download high resolution image](#)

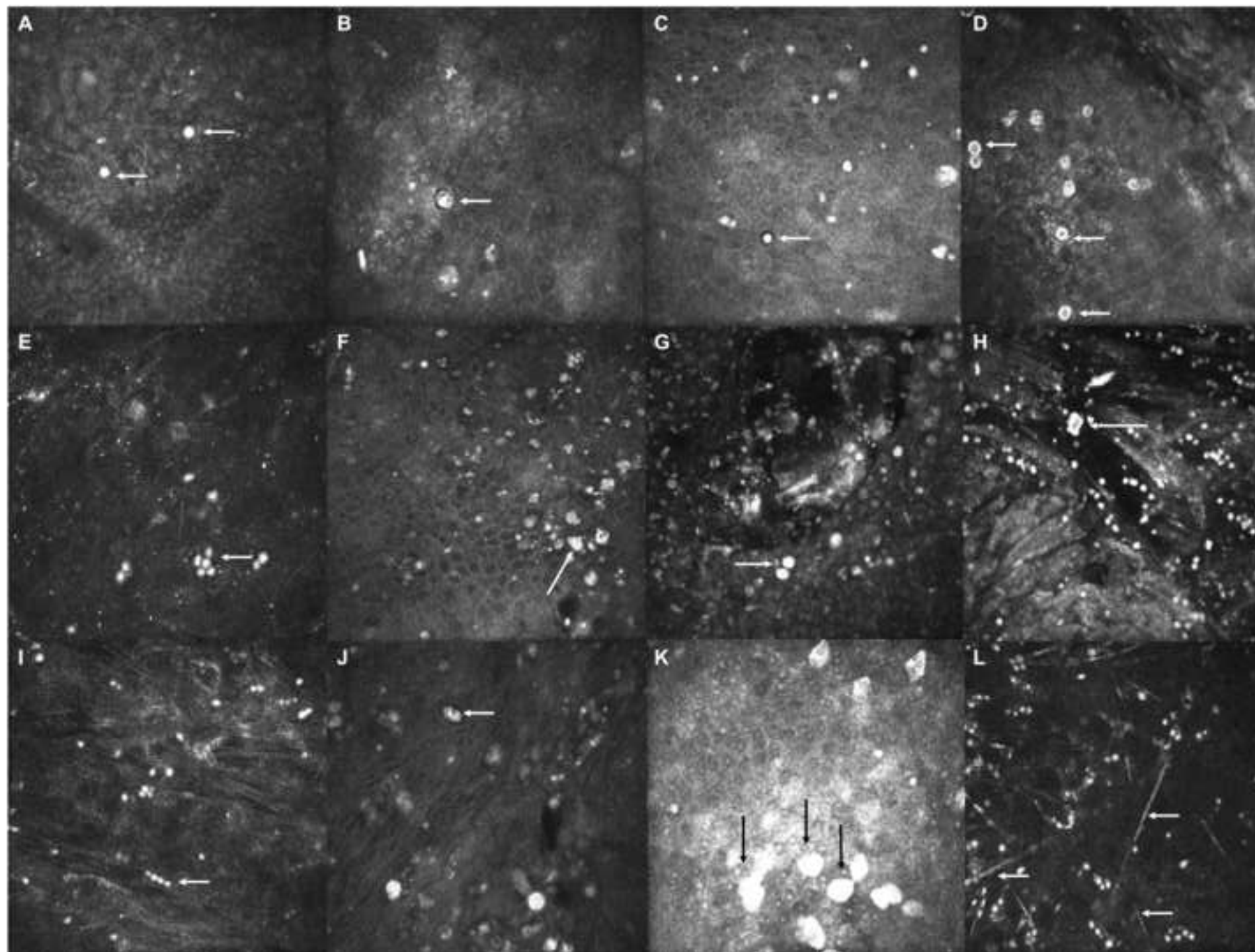


Figure 2
[Click here to download high resolution image](#)

